Can Airless Tyres Eliminate Caravan Fishtailing?

(Dr) Edward Brell BSc MEng PhD

Brisbane 4503, Australia
*Email: dredward@live.com.au
Phone: +61732045105; Mobile +61413824447

ABSTRACT

A tyre blow-out on a caravan can be disastrous, even fatal in severe situations. A non-pneumatic wheel (NPT) has the obvious advantage of being resistant to the DREADED FLAT TYRE. Thus, there is promise of safety. A number of tyre manufacturers have been busy developing a tyre or complete wheel to capitalize on this benefit. The best-known NPT is dubbed the TWEEL®. The nomenclature of Michelin's NPT is a joining of parts of the two words, *Tire* and *Wheel*. The TWEEL® has application to skid-steer loaders and commercial lawn mowers. Michelin encountered problems in the development of the TWEEL® for high speed use. One of these problems encountered by Michelin in the development of the Tweel may be a god-send for caravan wheels as they develop their new NPT for highway use. The design of the so-called UPTIS® is not just an improved version of the TWEEL® but a completely different operating philosophy. This paper considers the evolution of the NPT and considers how it might be beneficial in the caravan context. To illustrate, a fishtailing tale to tell gets told.

***Keywords**:* Caravan, fishtailing, snaking, UPTIS, TWEEL, NPT "non-pneumatic", airless.

INTRODUCTION

The aspiration to improve on air inflated tyres goes back a long, long way. Carl Purdy writes in his patent filed in 1904 (Purdy, 1905) as below. ***Figure 1*** refers.

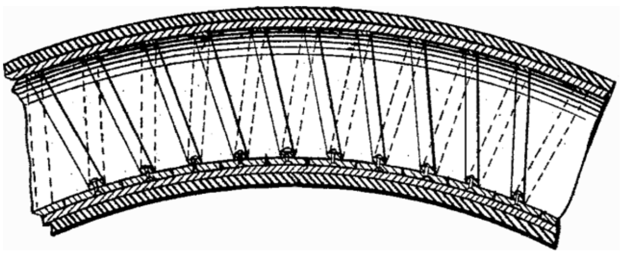

Figure 1 – Purdy's Spiral Spring Airless Tyre Patent

> *"This invention relates to tires, and more particularly to the class of cushion-tires, and has for its object to provide a tire which will be extremely resilient and in which the disadvantages common to pneumatic tires will be eliminated."*

Many inventions have been lodged since then and so far, only the TWEEL® has had marketing success. We must wait until 2024 before the first high speed airless tire rolls out of a General Motors (GM) production line for a highway speed use. "…probably not sooner than that." according to Steve Cron, senior principal product engineer at

Michelin. He added that they have a very high lateral stiffness. (Cole, 2019). It is the latter comment by Steve Cron that has implication for caravan fishtailing.

As an overview on tyre performance generally, the National Highway and Traffic Safety Authority (NHTSA) indicate failure of a tire/wheel was the most frequent critical reason for a vehicle crash. (NHTSA, 2008). Ramesh, (2020) quotes statistics of 738 deaths from 78,000 automobile crashes each year in the USA.

In a press release Michelin, (2020) report on their "Scrapyard Survey" taken over a period spanning 2 years viz. 2013-2015, as follows:

- 12% of tyres fail due to blow-outs.
- 8% fail due to irregular tyre pressure.
- Amounting to 200 million such tyres each year.
- In total an extrapolated 1 Billion tyres are scrapped each year world-wide.

It is not surprising therefore, that there is an urgent move to migrate towards tyres that do not require inflation. These statistics also show the potential to reduce raw materials use and waste. Michelin's UPTIS® and TWEEL® both non-pneumatic tyres, seed into a mission to conserve. The TWEEL® found success among low speed vehicles and more recently in NASA's latest lunar rover vehicles. Currently, non-pneumatic tyres are authorized for highway use only as a spare wheel according to rules by NHTSA, (1990). The UPTIS® is the hope for the next generation airless tyre to suit high speed vehicles.

The UPTIS® in
Figure 2 might look to be *fait accompli* on the press-release photographs, but unfortunately, the finished product, the result of a partnership between GM and Michelin might be different, only promising to show fruit in the year 2024. The challenges are significant. The aim of this paper is to understand some of these challenges in the context of safer caravanning.

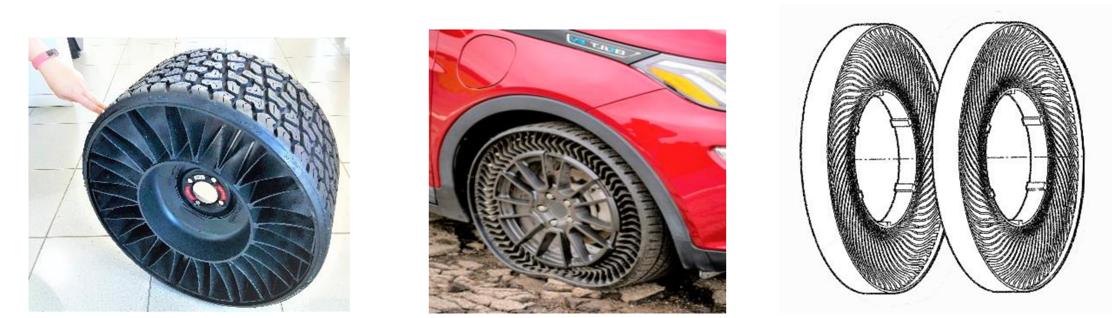

TWEEL ON SHOWROOM FLOOR UPTIS AS A FRONT WHEEL BRIDGESTONE HALVES

Figure 2 - Comparison – TWEEL®, UPTIS® & Bridgestone Airless Tyres

Little is known regarding the Bridgestone NPT

THE NON-PNEUMATIC TYRE

The non-pneumatic tyre (NPT) comprises a rigid hub that gets bolted to the vehicle axle stub, just like any other wheel. Radiating from the hub are elastomeric spokes that collapse to facilitate a ground engaging patch. Surrounding the spokes, one finds a ring serving as a so-called shear beam. Since the spokes offer little support for the hub in compressive mode, the upper spokes do the work in tension. The weight carried by the hub effectively hangs from the circular shear beam. Steve Cron (Michelin engineer) recalls explaining (Meyer, 2018): "The ground is not pushing directly to the bottom of your wheel. In the automobile, you should think of the tire as hanging." ***Figure 3*** refers showing the weight carried by three springs and the corresponding ground reaction.

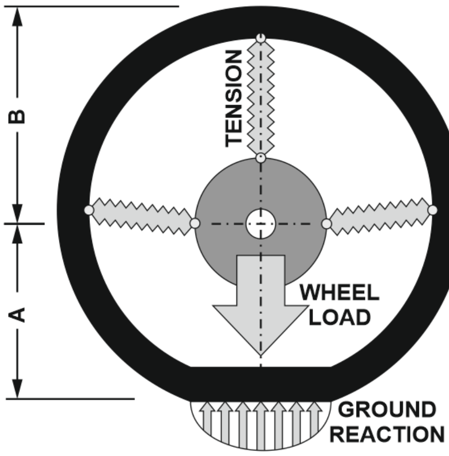

Figure 3 – Hanging weight principle of tyres

We test the hanging principle in ***Figure 3*** on a random pneumatic tyre by measuring the upper tyre radii for various inflation pressures. Obviously, such an exercise is not feasible on an NPT as there is no inflation pressure to vary.

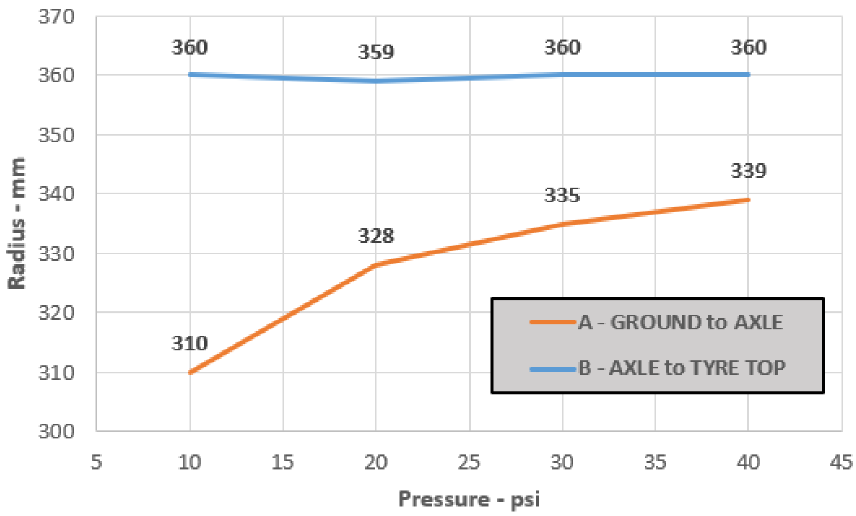

Figure 4 – Pneumatic tyre hanging dimensions

With the exception of the 20-psi measurement (likely the result of rounding convention) there was no axle droop from the top of the tyre.

STRUCTURAL vs GEOMETRIC STIFFNESS

A pneumatic tyre from the manufacturer comes with some structural stiffness that enables convenient handling, fitment and storage. This stiffness is obviously not sufficient for motoring hence the need for inflation. The geometric stiffening process can be visualized by inflating a bicycle inner tube. Before inflation it may lie completely flaccid on the table. However, even a small inflation pressure will bring it to life as a circular (almost) object as shown in ***Figure 5***.

Figure 5 – Bicycle inner tube demonstrating geometric stiffness.

Geometric stiffness in a pneumatic tyre is similarly achieved by the inflation pressure while the non-pneumatic shear beam must develop stiffness by virtue of structural shear and bending resistance. Geometric stiffness also applies to natural frequencies of vibration as shown by (Jia et al., 2005). We visualize the increase in mode shape stiffness for a P195/60R14 tyre from their data in ***Figure 6***:

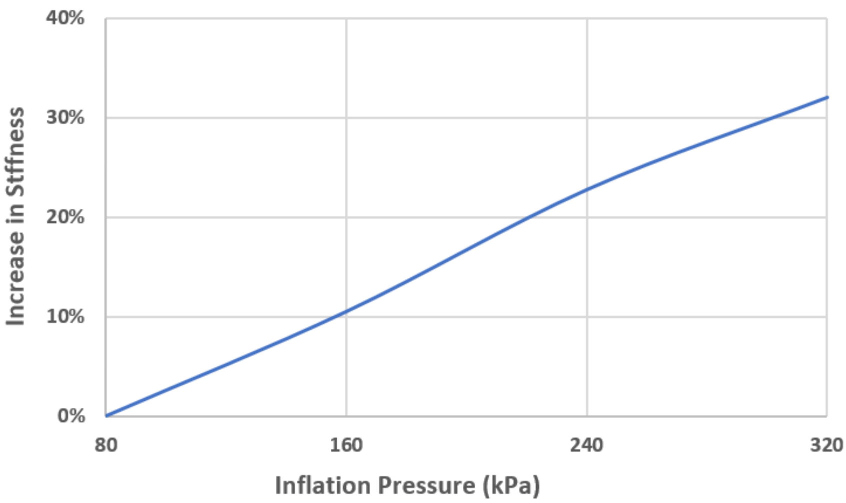

Figure 6 – Increase in vibration stiffness due to inflation pressure.

LATERAL STIFFNESS

Lateral stiffness can be defined as the force required to deflect the tyre sideways. Brell & Thambiratnam, (2020) compared two identical outside diameter tyres; one of low lateral stiffness and the other high lateral stiffness. The high lateral stiffness tyre showed a significant improvement in fishtailing energy thus lessening the severity of such an event. Lateral stiffness in a caravan tyre is a very desirable thing.

The shear beam or tread band on a tyre must have significant structure to support the hanging axle load. Unfortunately, the NPT shear beam, as we currently know it, can perform (i.e. hold the axle up) only if it has structural stiffness. Thus, it must have adequate section modulus to resist collapse yet not too stiff to allow an adequate contact patch to form with the ground. A large section modulus is associated with high lateral stiffness, the sought-after feature for caravans.

To perform some testing, Michelin equipped an Audi A4 with five times the lateral stiffness as normal. The result was reported by Michelin as "responsive handling". (Mihalascu, 2010)

Towing a caravan with tyres having a high lateral flexibility (i.e. low lateral stiffness) should be thought of as towing a drawbar-equipped shopping trolley – an invitation to sway wildly at every lane change. By way of contrast, laterally stiff tyres on a tandem axle or tri-axle could encourage dangerous oversteer in the towing vehicle, especially on, say, a downhill curve where drawbar steer might control flexible car rear tyres. While high lateral stiffness on a tri-axle may exacerbate tyre wear slightly, there appear no such downsides on single axle towing.

Against the significant benefit of never having a flat tyre, must be weighed the amount of TWEEL® noise and just how bad the TWEEL® vibration might be. There appear no noise and vibration test reports in the literature. Manga, (2008) recommended in his further research section, the following:

- Apply strain gages to TWEEL® spoke and run on a chassis dyno in an anechoic chamber.
- Use slip-rings to get signals out.
- Record acoustic signal in vicinity of TWEEL® at a range of speeds.

It appears the foreshadowed research has not materialized.

NOISE, HEAT & VIBRATION

Steve Cron had already tested the TWEEL® on public roads. "I had it on my car," he said. "I drove every day for four years" according to the interview by Craig Cole. (Cole, 2019). Cron reported no issues at the time but it is generally known that the TWEEL® does have issues at the higher speeds. (Raiciu, 2009). Cron conceded at the 2010 Simulia Customer Conference: "One of the challenges in TWEEL® tire development has been the noise and vibration caused by the TWEEL® tire, rolling at speeds typical of an automobile." (Cron, 2010).

Manga (2008) postulated the noise and vibration emanated from spoke flapping as a result of spoke buckling then retensioning. Using Finite Element Analyses (FEA), spoke vibration was demonstrated at identical frequencies both at 60 and 80 km/h leading to a conclusion that the spokes will vibrate at their resonant frequency independent of rolling speed.

One might ask whether the noise and vibration matter in the caravan context given the remoteness of occupants.

In what appears a securing of patent protection, a modification was claimed in a patent by Delfino et al. (2017). The reduced lateral stiffness is accomplished by reducing the overall width of the shear panel of the spoke as well as a slit that separates the spoke panel into two or more (as claimed). Here lateral stiffness is seen as a problem to be solved. The sketch in ***Figure 7*** refers.

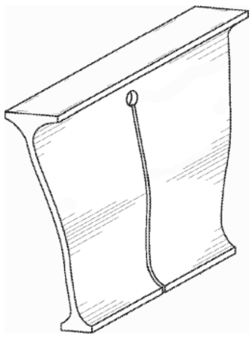

Figure 7 – Web shear strength reduction.

One of the problems preventing the TWEEL® from becoming a high-speed tyre was vibration. Vibration is influenced by the two parameters: mass and stiffness. Clearly, the TWEEL® needs a stronger and heavier shear beam to support the hanging axle than is needed for the UPTIS®. There are many mode shapes in the vibration responses in any tyre. A full comparison of vibration on these two tyres is beyond scope for this paper. However, one mode shape stands out and could well be in frequency range of resonance. This is visualized in ***Figure 8*** where the size of oscillating mass is a relevant feature.

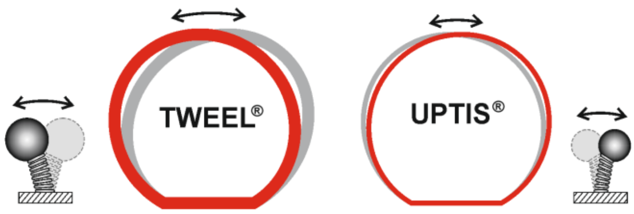

Figure 8 – Vibration mode shape comparison – in analogy

The lesser mass in the UPTIS® shear beam emphasizes one of the advantages of bottom support as against hanging support found in the TWEEL®.

…all of which helps to appreciate the finesse of the UPTIS® design in the details to follow.

CLEVER UPTIS®

Whilst it was intended for automobiles (Rhyne et al 2001), there appears an abandoning of the TWEEL® of ever becoming a high-speed airless tyre. The UPTIS® appears not to be just an upgrade on the TWEEL®. Rather, it represents a complete departure from the hanging principle shown in ***Figure 3***.

Performance of the UPTIS® is dependent both on the material properties and the geometry of the structure. Little is published regarding UPTIS® other than marketing hyperbole in press releases. These are mostly of little value in an engineering sense. The rendering of physical embodiments in patent applications is an area of great interest in understanding the product under development, especially when speculating on an extension to their immediate intent and usefulness.

Fortunately, Michelin patents give some insight, since disclosure of details is a precondition of the granting of a patent. Study of progression of their patents also give insight. One such Michelin patent, (Miles et al., 2019) shows a row of spring steel spokes encased in an elastomer-like polymeric. The encapsulated spoke flexes in response to the formation of a contact patch.

As the wheel rotates the spokes make contact with adjoining non-flexing portions of the spokes (mounting bases) so changing the lengths of spokes in flexure. ***Figure 9*** shows a tracking of a single spoke through-out the flattening of the contact patch. The progress is as follows:

- The spoke is approximately the shape as shown on the End View of ***Figure 9***
- and may possibly be unflexed, pre-stressed or pre-tensioned at the point of entry into the contact patch affected zone.
- At this point, the starting point of this description, R_0 is considered the natural spring rate of the spoke.
- R_1 is the spoke's spring rate when the top end of the spoke is held in place by the top mounting base and the spoke length is shortened by the support of the adjoining spoke mounting base.

- The spoke progresses to where it is again shortened by contact with both top and bottom adjoining mounting bases. Here the spring rate is R_2 representing the shortened spring length in flexure.
- The spoke under consideration is now leaving the contact patch affected zone still having support at the top adjoining mounting base reducing the spring rate to R_3.
- Beyond the affected zone the spoke now reverts back to R_0.
- The spring rates are not only affected by the spoke's stiffness, as varied positionally, but also by the flexure of the adjoining mounting bases.
- 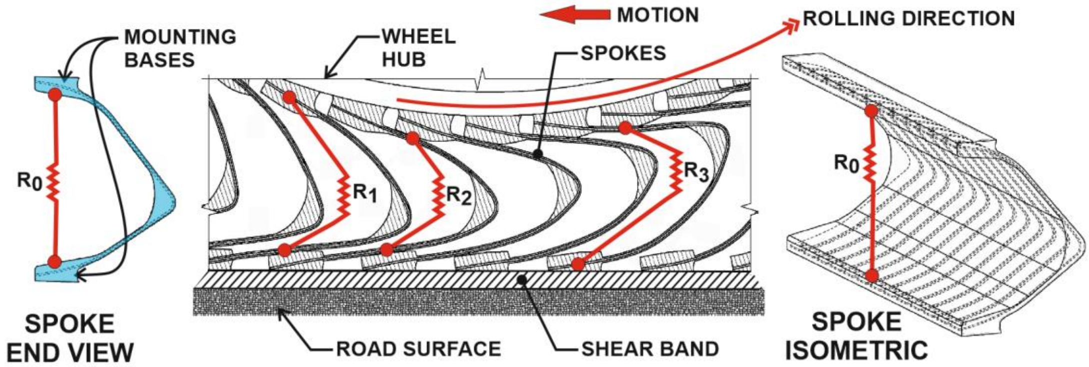

Figure 9 – Flexing of spokes showing changing spring rates

In the description above it can be seen that the application and release of forces to support the wheel hub, although rapid, is a gentle and progressive process.

Since lateral tyre stiffness is the mainstay of this paper to minimise fishtailing of caravans, it is competent to discuss the mechanics of stiffness to be delivered by the UPTIS®, if only to demonstrate the adaptability of the UPTIS design.

It is tempting to ascribe such stiffness to St Venant's torsion of the cross-section since superficially it appears like the spoke is in simple shear. This is shown in ***Figure 10*** where a force ***(F)*** causes a shear displacement ***(D).***

There are 13 spring steel elements in the spoke of ***Figure 10*** according to their patent. Although the element is encastered in a flexible matrix of an elastomer, each element plays a part in the overall lateral stiffness of the spoke. Although the flexible matrix plays a part in the overall lateral stiffness, we study the spring steel elements in isolation (as if the elastomer were not present).

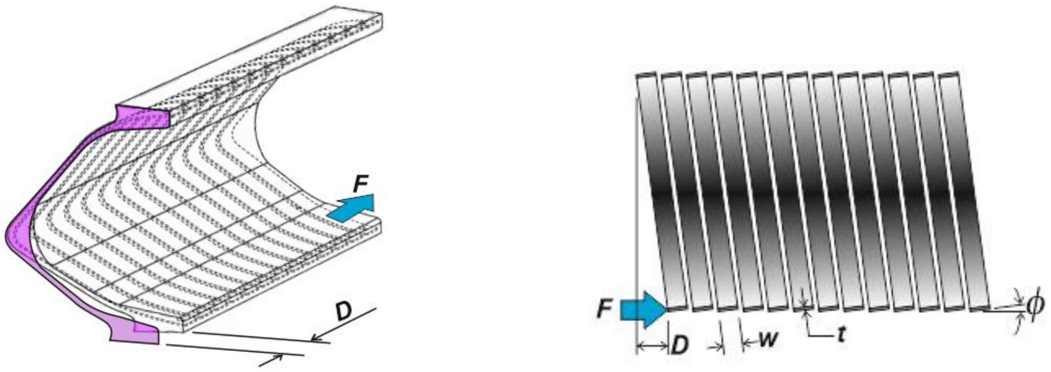

Figure 10 – Shear displacement of spoke – Isometric & Elevation Views

It will be noticed that in ***Figure 10*** an angle is subtended designated $\boldsymbol{\phi}$**.** Since each strip is fixed top and bottom, this angle becomes zero and causes twist. Classical St Venant torsion can be used here using moment of resistance in lieu of polar moment of inertia. Moment of torsional resistance can be calculated (approximately) from Equation **1**:

$$\boldsymbol{M_T} = 0.3\ x\ w\ x\ t^3 \quad \textbf{\textit{Equation 1}}$$

To understand the behaviour of the spring steel element better, a strip of 200 gsm paper was arranged on two pieces of string, vertically separated. This is shown in ***Figure 11***.

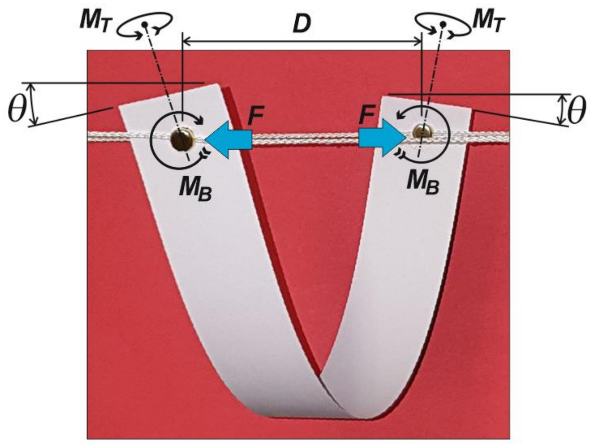

Figure 11 – Lateral stiffness of strip element.

The end fixity of the strip in (if it were in an UPTIS®) requires the angle $\boldsymbol{\theta}$ to be zero, thus develop the moment $\boldsymbol{M_B}$. This, in turn creates bending of double curvature visualized as a beam in ***Figure 12***:

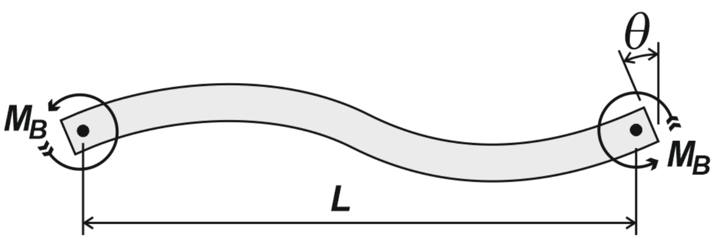

Figure 12 – Bending stiffness of strip element.

Transposing Bending Equation 1(f) from Table 8.1 Roark's Formulas for Stress and Strains (Young & Budynas, 2002) yield a relationship for the bending moment in Equation 2. Both moments ($\boldsymbol{M_T}$ and $\boldsymbol{M_B}$, Equation **1** &Equation **2**) are a product of strip width ***(w)*** and strip thickness ***(t)***. An increase in either will increase lateral stiffness. Only a small mathematical manipulation is needed, (remaining for future work), to arrive at the classical rendition of stiffness (***F/D*** = N/mm). Sufficient for this paper's aims to conclude that both St Venant's torsion and bending across the strong axis of strip are implicated in lateral stiffness of the UPTIS®.

To produce a stiffer UPTIS® all that is needed is a smaller number of strips but wider to acquit the same vertical stiffness needs.

To conclude on the UPTIS® here, there is hope for a future lateral very stiff NPT becoming available in the market place.

To summarize on the importance of tire performance we quote Kurtz & Anderson, (1977):

> *"In the hierarchy of forces acting upon cars towing trailers, it is generally agreed that the tire forces exerted on the vehicle by the road are of primary importance. Anyone embarking on a study of the handling characteristics of such vehicles would thus be wise to pay considerable attention to tire forces."*

Next we reflect on the words of Fratila & Darling, (1996) seemingly expressing surprise that the modelling did not agree with testing:

> *"Differences in results were attributed to factors not included in the computer simulation such as tyre lateral stiffness…"*

Finally, we lament the absolute dearth of lateral stiffness values tested and published by tyre manufacturers.

A FISHTAILING TALE TO TELL

Forensic examination of a real-life event has permitted extraction of useful oscillation details. Whilst there are many videos posted on the Internet showing caravans towed to destruction, one Internet posting is of a caravan rig that was successfully stopped without damage. (Note the tail lights in ***Figure 13***). This posting was of particular value since shadow cast on the roadway were sharply defined permitting some graphical solutions to be derived. A dashcam video of the event was posted on YouTube and can be viewed here:

https://www.youtube.com/watch?v=qo-qpy0krkE

Figure 13 – Stills from dashcam video (Sequence L to R)

In the dashcam video, the 4WD towing the caravan was overtaking a truck on a dual carriageway down a slight downward incline, getting into difficulty, according to Harvey Day, (2017). The speed limit for caravans on that road was 60 mph. It is hard to imagine that a truck driver would be much under 60 mph on a clear downhill run. Thus, the 4WD must have been exceeding the speed limit to be overtaking.

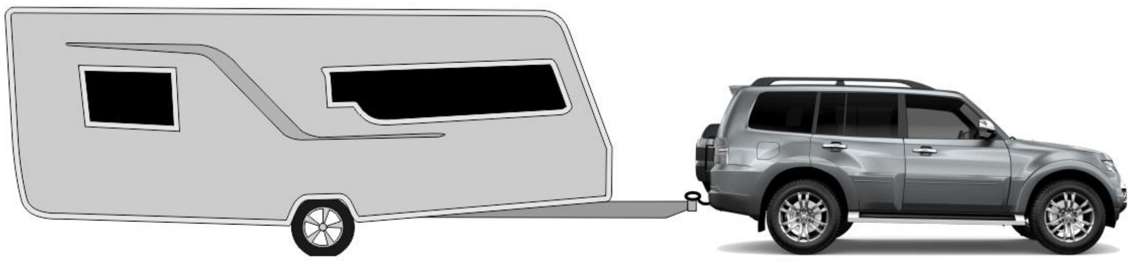

Figure 14 – Vehicles involved in fishtailing event on the A30 into Cornwall UK.

Some specifications for the vehicles in ***Figure 14*** can be found in ***Table 1***.

Table 1 - Specifications of Vehicles

Vehicle	**Argosy**	**Shogun**
Drawbar (Scaled)	W_B=3.88m	-
Overall Length	*Long=6.347m*	*4900mm*
Width	*Wide=2.286m*	*1875mm*
Wheelbase	-	*2780mm*
Weight	*M=1448 kg*	*2375 kg*
Two Tyres	*185 x R14*	

Whether the Shogun driver made his lane change too rapidly (the truck driver reported a clipping of his wing mirror), or the interaction of the caravan with the truck bow wave started the oscillation, are not known. It is also possible that the Shogun exceeded critical velocity above which instability can occur. Critical velocity can be determined according to (Genta & Genta, 2017):

$$V_{CR} := \frac{1}{2} \cdot \sqrt{\frac{C \cdot W_B{}^3}{J_H}}$$ ***Equation 3***

Where cornering Stiffness © is extrapolated from data published for a 185 x R14 tyre by Cabrera et al., (2005) and posted to ***Figure 15***.

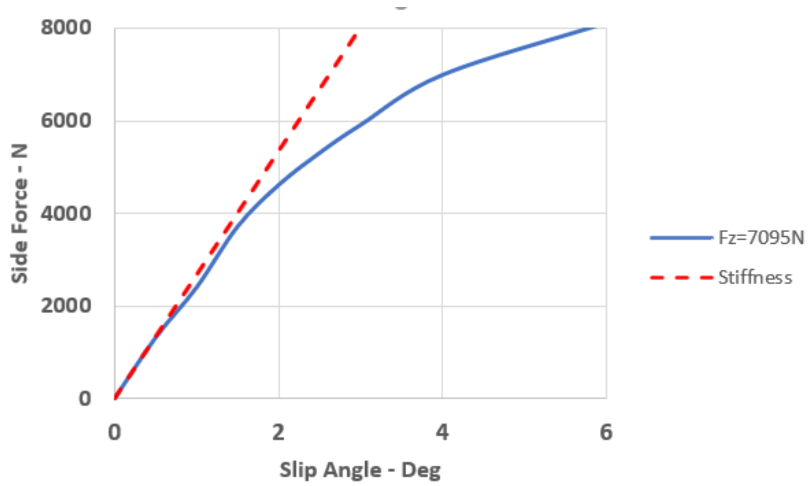

Figure 15 – Cornering stiffness extrapolated from data by Cabrera et al., (2005).

Thus cornering stiffness is calculated for a single axis caravan as 5333 N/deg for the total of two of these tyres.

Some assumptions are needed:

- A straight-line hitchpoint path is assumed.
- Start of sequence is from a nominal point after the Shogun first appears.
- Finish of sequence is at jack-knife.
- Length of sequence considered is 9 seconds.
- Road width is 7.0 m
- Weight is evenly distributed and centred on intersection of axle and drawbar.
- Centroidal mass moment of inertia of caravan is calculated as evenly distributed.
- Hitchpoint mass moment of inertia is calculated by the parallel axis theorem.

The peak angles of articulation are determined by rotating shadows into the true vertical plane to the procedure shown in ***Figure 16***:

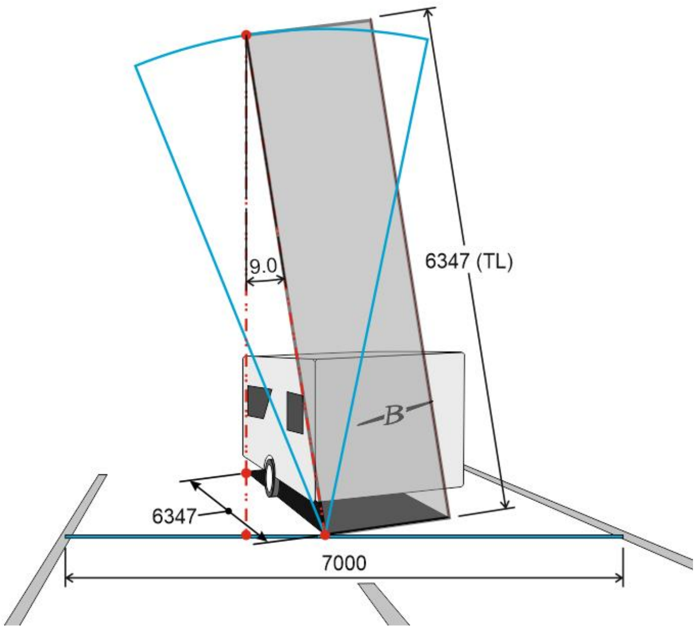

Figure 16 – Rotating shadow to extract true articulation angle

The peak articulations graphed together with those estimated, are plotted against the sequence time from the video to ***Figure 17***:

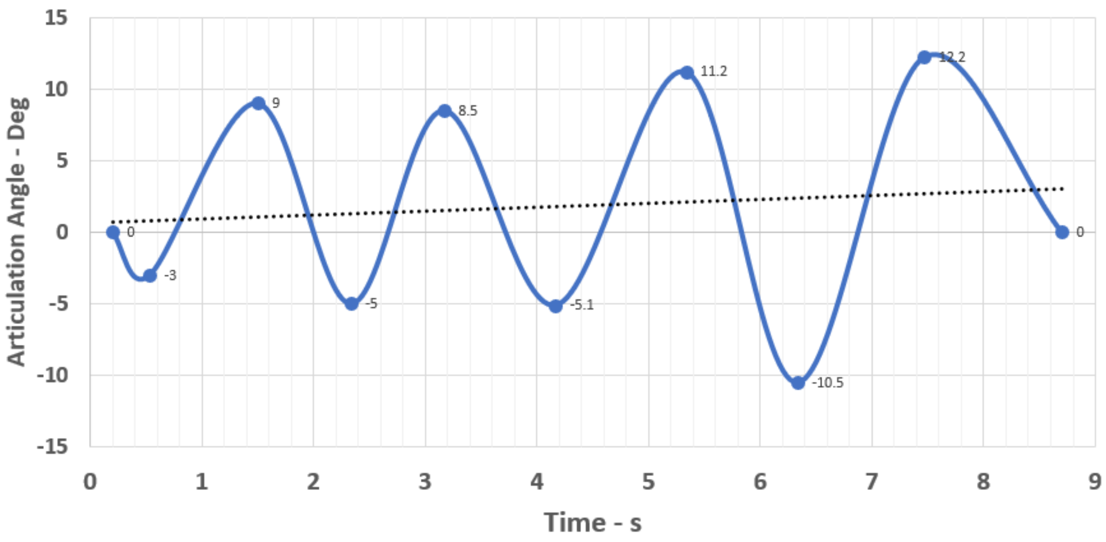

Figure 17 – Transient articulation angles.

The start and finish data points were estimated while the radii at the data peaks are added by the spreadsheet software. The dotted trend line corresponds with the general direction of hitchpoint travel. This line better represents the zero-articulation point in the oscillation.

To reflect this ***Figure 17*** is redrawn, the dotted line as the abscissa. ***Figure 18*** refers. Here it can be noted that even though towards the end the estimated caravan speed is clearly below the critical speed, the sway angle of the caravan increases.

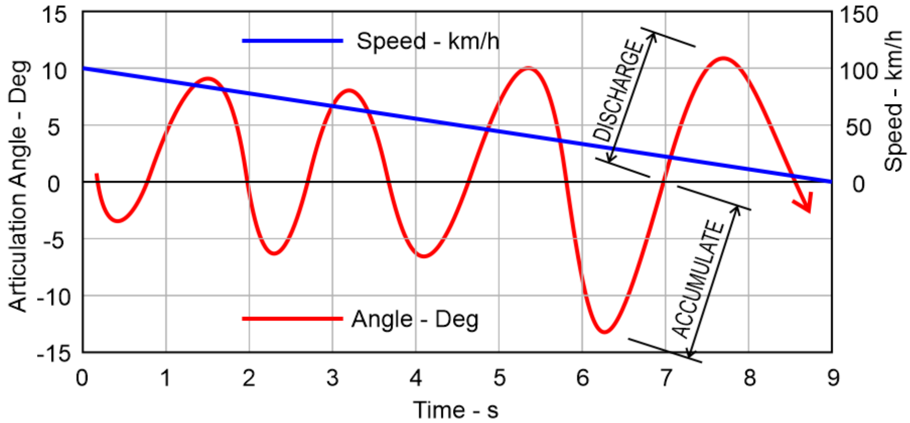

Figure 18 – Adjusted articulation angles showing speed decay & yaw energy exchange.

At each oscillation there is a phase where rotational kinetic energy is built up, to be acquitted subsequently by a discharge phase. When so-called yaw energy exceeds the level of damping a wider sway occurs. This can be observed in ***Figure 18*** where the sway angles increase to above 10^{O}.

It would be instructive to compare the yaw energies involved in the oscillation cycles in the radial tyres as fitted, to the TWEEL®. Unfortunately, a complexity manifests. Yaw energy is not even through-out its accumulation stroke. Here, we must agree with Pacejka & Sharp (1991) where accuracy must sometimes yield to demands of complexity. Thus, yaw energy is calculated based on average yaw velocity.

We invoke Walt Disney's 'plausible-impossible' (Beaudine & Jackson, 1956) and freeze-frame at 1.5.seconds into the fishtailing sequence to change tyres and complete the remainder of the journey on tyres that have no sideslip. Perhaps the TWEELS as fitted to the BMW (having 5X lateral stiffness) as reported in (Mihalascu, 2010) were as stiff. We will assume so. An accumulation phase could then be replaced with a tractrix to represent the BMW Tweel®. This is shown in ***Figure 19***:

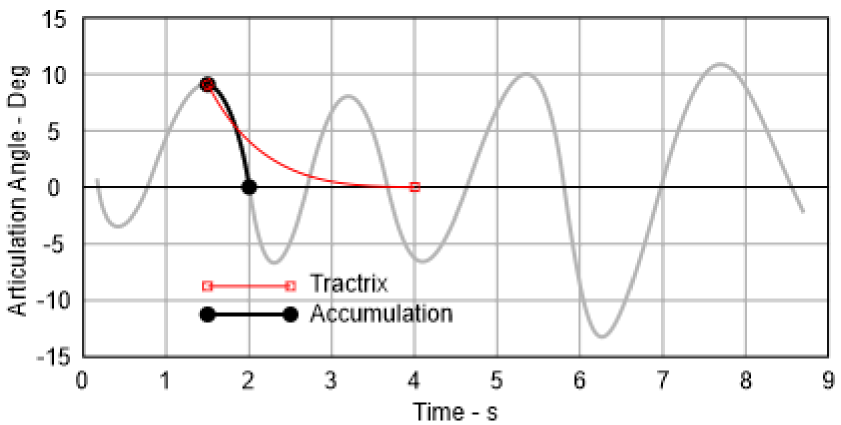

Figure 19 – Accumulation phase replaced with notional BMW Tweel®

The old tyres achieved a yaw displacement of 9.4^{O} in 0.5 s giving a yaw rate of 18.8 deg/s. The notional BMW Tweel® takes 2.5 s to wash off the same articulation angle of

9.4^{O} giving a mere 3.8^{O} /s yaw rate. There are clear implications for the yaw energy to be acquitted in the discharge phase, as follows in **Table 2**:

Table 2 – Radial vs TWEEL®

Item	Radial	TWEEL®
Angular Velocity (Average)	$\omega_R := 18.8 \frac{deg}{s} = 0.328 \frac{rad}{s}$	$\omega_T := 3.8 \frac{deg}{s} = 0.066 \frac{rad}{s}$
Critical Velocity (Equation 3)	$\frac{1}{2} \cdot \sqrt{\frac{C \cdot {W_B}^3}{J_H}} = 49 \frac{km}{hr}$	$\frac{1}{2} \cdot \sqrt{\frac{(5 \cdot C) \cdot {W_B}^3}{J_H}} = 109 \frac{km}{hr}$
Kinetic Rotational (Yaw) Energy	$Y_R := \frac{1}{2} \cdot J_H \cdot {\omega_R}^2 = 1306\ J$	$Y_T := \frac{1}{2} \cdot J_H \cdot {\omega_T}^2 = 53\ J$

Driving at speeds above the critical velocity does not mean that fishtailing necessarily occurs. It simply refers to an instability zone. A caravan rig needs initiating factors for fishtailing to manifest. There appear to be a number of these factors present in this fishtailing tale such as lane changing, truck bow wave, speed and overtaking.

Then again, it might be that the tyres were just inadequate for the task. The huge difference in the calculated yaw energies support this idea.

DISCUSSION

The promise of never having a flat tyre holds appeal. So too, never having to check tyre pressure. For a caravan, these are very good things, especially given the many days a caravan typically spends at home idle.

The prototype Chevrolet Bolt EV is to offer the UPTIS® sometime in 2024 or beyond. According to the specification sheet, this car tares at 3,563 lbs, or about 400 kg average tyre load. There is little choice of available caravan models at 800 kg tare or 1,600 kg tare for a tandem axle, thus limiting the proposed tyre specification for caravan use.

Further, the UPTIS® photos from the press releases show 64 spokes per tyre. Each spoke having 13 spring steel elements according to the patent diagrams. To outfit the BOLT requires a staggering 3,328 spring steel elements. This, in an industry extremely sensitive to even a single unnecessary washer. Fortunately, it does not need a spare tyre so avoiding another 832 elements.

Notwithstanding, the air pumping action of the knee-shaped spoke should keep the UPTIS® tyre cool and so extend its service life. Then too, there is scope to provide greater lateral stiffness to the rear tyres for perfect directional control by the Bolt EV. Then there may be scope for a bigger specification for future outfitting, say, GM's Hummer model. Given the military predilection for this model, there is the hope for caravans in the foreseeable future.

As for eliminating fishtailing altogether? Routine publication of tyre lateral stiffness by tyre manufacturers would be a good starting point. Failing that, a run-flat tyre of the type that has stiffened sidewalls might be an option. A comparison of normal tyre with a run-flat tyre is compared in ***Figure 20***:

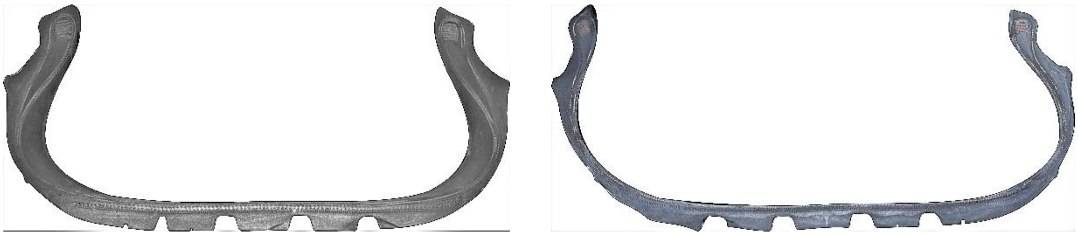

Figure 20 – Cross-section of run-flat tyre (left) compared with normal tyre (right)

REFERENCES

Beaudine, W., & Jackson, W. (1956). *The Plausible Impossible*.

Brell, E., & Thambiratnam, D. (2020). Tyre Contribution to Caravan Fishtailing. *International Journal of Automotive and Mechanical Engineering (In Peer-Review)*.

Cabrera, J., Ortiz, A., Carabias, E., & Simon, A. (2005). Experience with the IMMa tyre test bench for the determination of tyre model parameters using genetic techniques. *Vehicle System Dynamics*, 253–266. https://doi.org/10.1080/00423110500140112

Cole, C. (2019). *Why GM and Michelin's airless Uptis is the future of car and truck tires*. Roadshow by CNET. https://www.cnet.com/roadshow/news/gm-michelin-uptis-airless-tires/

Cron, S. (2010). Role of Abaqus in the Development of the Michelin Tweel® Tire. *2010 SIMULIA Customer Conference*.

Day, H. (2017). *Heart-stopping moment 'out-of-control'caravan*.

Delfino, A., Berguerand, P., Schroeder, P., Cron, S., & Rhyne, T. (2017). *NON-PNEUMATIC WHEEL* (Patent No. WO 2017/117598 Al).

Fratila, D., & Darling, J. (1996). Simulation of Coupled Car and Caravan Handling Behaviour. *Vehicle System Dynamics*, *26*(6), 397–429. https://doi.org/10.1080/00423119608969317

Genta, G., & Genta, A. (2017). *Road Vehicle Dynamics: Fundamentals Of Modeling And Simulation* (1st ed.). World Scientific.

Jia, L., Xu, Y., & Zhang, J. (2005). Free vibration analysis of radial pneumatic tires. *Journal of Sound and Vibration*, *285*, 887–903.

Kurtz, E. F., & Anderson, R. (1977). Handling Characteristics of Car-Trailer Systems. *Vehicle System Dynamics*, *6*, 217–243.

Manga, K. (2008). *Computational Method for Solving Spoke Dynamics on High*. Clemson University.

Meyer, B. (2018). Long development journey pays off for Tweel, Michelin. *Rubber & Plastic News*. https://www.rubbernews.com/article/20181017/NEWS/181019944/long-development-journey-pays-off-for-tweel-michelin

Michelin. (n.d.). *Air out of Tires*. 2020. Retrieved July 30, 2020, from https://michelinmedia.com/michelin-uptis/

Mihalascu, D. (2010). Reinventing the Wheel: a Guide to Michelin's Airless Tire. *Autoevolution*. https://www.autoevolution.com/news/reinventing-the-wheel-a-guide-to-michelins-airless-tire-19937.html

Miles, K., Cron, S., & Thyne, T. (2019). *NON-PNEUMATIC TIRE CARCASS* (Patent No. WO 2019/089008 A1).

New Non-Pneumatic Tires for Passenger Cars, (1990).

NHTSA. (2008). *Traffic Safety Facts: The National Motor Vehicle Crash Causation Survey* (Issue December). https://crashstats.nhtsa.dot.gov/Api/Public/ViewPublication/811059

Pacejka, H., & Sharp, R. (1991). Shear force development by pneumatic tyres in steady state conditions : a review of modeling aspects. *Vehicle System Dynamics*, *20*(3–4).

Purdy, C. (1905). *Tire* (Patent No. 795732).

Raiciu, T. (2009). *History of the Wheel*. Autoevolution. https://www.autoevolution.com/news/history-of-the-wheel-7334.html

Ramesh, H. (2020). *The Race to develop Airless Tires*. GAVOP. https://www.gavop.com/b/race-develop-airless-tires-top-companies-cm1154/

Rhyne, T;Thompson, R;Cron, S;Demino, K. (2001). *NON-PNEUMATIC TIRE* (Patent No. WO 03/018332 A1).

Young, W., & Budynas, R. (2002). *Roark's Formulas for Stress & Strains* (7th ed.). McGraw-Hill.